Hydrogel Nanoparticles with Covalently Linked Coomassie Blue for Brain Tumor Delineation Visible to the Surgeon

*Guochao Nie, Hoe Jin Hah, Gwangseong Kim, Yong-Eun Koo Lee, Ming Qin, Tanvi S. Ratani, Panagiotis Fotiadis, Amber Miller, Akiko Kochi, Di Gao, Thomas Chen, Daniel A. Orringer, Oren Sagher, Martin A. Philbert, and Raoul Kopelman**

***D**elineation of tumor margins is a critical and challenging objective during brain cancer surgery. A tumor-targeting deep-blue nanoparticle-based visible contrast agent is described, which, for the first time, offers in vivo tumor-specific visible color staining. This technology thus enables color-guided tumor resection in real time, with no need for extra equipment or special lighting conditions. The visual contrast agent consists of polyacrylamide nanoparticles covalently linked to Coomassie Blue molecules (for nonleachable blue color contrast), which are surface-conjugated with polyethylene glycol and F3 peptides for efficient in vivo circulation and tumor targeting, respectively.*

1. Introduction

For many forms of cancer, surgery is an essential treatment modality. The precise delineation of tumor margins and subsequent complete surgical resection, without damaging crucial structures near the tumor bed, is one of the great challenges in brain tumor surgery.[1] The extent of tumor resection relies on the precision of tumor delineation and affects the length and quality of survival for the cancer patient.[2] In current clinical settings, resection of the tumor is guided by preoperative imaging studies, along with the operating surgeon's ability to distinguish the lesion grossly by its appearance and consistency, with respect to normal tissue, which, by itself, is not reliable enough to achieve complete resection. In particular, brain tumor tissue, which is easily detected radiographically, may be virtually indistinguishable from normal brain tissue in its visual appearance.

Various attempts for improvement of tumor delineation during brain tumor surgery have been made, based on two types of approaches: 1) implementing medical imaging instrumentation, and 2) applying fluorescent or visual contrasting reagents. The first approach includes the implementation of image-guided stereotactic navigation[3] and intraoperative magnetic resonance imaging (MRI).[4] These high-tech instrumentation-aided techniques have been used in the clinic and can greatly improve the accuracy of surgery. However, their use still has various restrictions, including possible reduced accuracy due to the practicing surgeon's divided attention between patient and monitor, longer setup time, high cost, limited availability, as well as poor instrument compatibility due to the necessity of having strong magnetic

Dr. G. Nie,[+] Dr. H. J. Hah,[+] Dr. G. Kim,[+] Dr. Y.-E. Koo Lee, M. Qin, T. S. Ratani, P. Fotiadis, A. Miller, A. Kochi, D. Gao, Prof. R. Kopelman
Department of Chemistry
University of Michigan
930 N. University Ave., Ann Arbor, MI 48109, USA
E-mail: kopelman@umich.edu
T. Chen, Dr. D. A. Orringer, Dr. O. Sagher
Department of Neurosurgery
University of Michigan
1500 E. Medical Center Drive, Ann Arbor, MI 48109-5338, USA
Dr. M. A. Philbert
School of Public Health
University of Michigan
1415 Washington Heights, Ann Arbor, MI 48109-2029, USA
Dr. G. Nie
Department of Chemistry and Biology
Yulin Normal University
Yulin, Guangxi 537000, China
[+] These authors contributed equally to this work.

DOI: 10.1002/smll.201101607

NANO MICRO small

fields within the operating space (intraoperative MRI). The second approach has been attempted by using fluorophores or visible dyes to stain tumor tissue. Fluorescein,[5] 5-aminolevulinic acid (5-ALA),[6] indocyanine green,[7] bromophenol blue,[8] and Coomassie Blue[9] have been suggested. In principle, dyes can preferentially stain malignant gliomas as they diffuse more readily across the areas of breakdown (fenestrations) of the blood–brain barrier. Although this approach allows surgeons to fully focus on the patient due to the visual contrasting effect coming directly from the tumor tissues, it is still subject to several limitations. For instance, fluorescence dye-based delineation requires special lighting and the elevated risk in performing operations in near darkness, as well as interruptions of surgery. In addition, a general drawback of dye-based delineation has been a lack of target specificity, systemic cytotoxicity, a requirement of intolerable high doses to achieve satisfactory visual contrast, and short-lasting retention at the desired site.[10]

The use of nanoparticles (NPs) may present a solution for overcoming the limitations of the currently proposed methods of dye-based tumor delineation, due to their several advantages, such as high loading of drugs and contrast agents, nontoxicity of the matrix, and selective tumor targeting, including passive targeting by the enhanced permeability and retention (EPR) effect and active targeting by a surface-conjugated, tumor-specific targeting moiety.[11] Iron oxide-based NPs tagged with the near-infrared (NIR) fluorescent dye Cy5.5 have been suggested as a method for dye-based intraoperative delineation of brain tumors.[12] However, one practical flaw of Cy5.5-tagged NPs is that, despite the deep tissue penetrating capability of NIR fluorescence, the NIR fluorescence of Cy5.5 is invisible to the naked eye and can only be visualized on a separate monitor. Our group has proposed an alternative approach, based on the brain-tumor-targeted delivery of a visual delineating reagent made of NPs.[13] We performed a preliminary proof-of-principle study on visual tumor delineation by using NP surface-conjugated F3 peptides for glioma targeting, with polyacrylamide (PAA) NPs containing the blue dye, Coomassie Brilliant Blue G-250 (CB).[13] CB turned out to be a very good candidate as a visible color contrast enhancer for intraoperative tumor delineation.[13] It has a vivid blue color in the pH 3 to 11 range, with a very high molar extinction coefficient.[14] It is also known to be safe for intravenous injection into the human body, even at very high doses.[15] However, our approach using the previously reported CB-loaded NPs still had a significant challenge with respect to application in vivo. Because the NPs were prepared by loading CB into preformed blank NPs by "physical" adsorption (termed "post-loading"), they produced a rather high degree of nonspecific cell staining with the passage of time (**Figure 1**),[10] which may lead to inefficient specific tumor staining in vivo.

Herein, we report significant improvements made to overcome the drawbacks of the preliminary approach, including: 1) development of a covalently linkable CB derivative to prevent unwanted premature dye leaching; 2) modification of the NP synthesis procedures to achieve sufficient dye loading by covalent linkage, and 3) introduction of polyethylene glycol (PEG)-containing crosslinkers for conjugation between

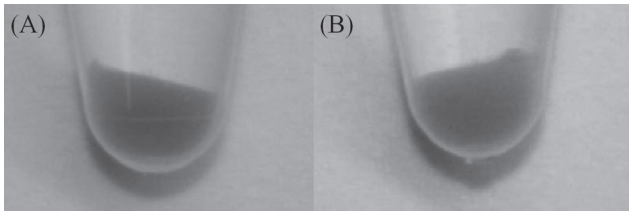

Figure 1. Significant nonspecific cell staining by dye leaching from CB-post-loaded PAA NPs. Brain tumor cells (9L gliosarcoma) incubated for 1 h with A) F3-targeted CB-post-loaded PAA NPs and B) nontargeted CB-post-loaded PAA NPs exhibit a strong positive blue staining effect regardless of cell binding of NPs by F3 targeting.

the NP and the F3 peptide, for improved stability in blood plasma and for preventing nonspecific binding. The new NPs, with covalently loaded CB, showed a highly selective blue staining of 9L glioma cells with negligible nonspecific staining in vitro, as well as selective tumor staining in vivo, in 9L-bearing rats with a cranial window, when compared with CB-post-loaded PAA NPs. The tumor-specific, nonleachable, blue-colored NPs do give good tumor delineation, which can be easily visualized by the naked eye, with enough contrast to potentially enable complete resection of the tumor with no extra equipment, no interruptions, and no unusual lighting conditions during surgery.

2. Results and Discussion

2.1. Synthesis of a Crosslinkable CB Derivative and its Characterization

As a first step to prepare CB covalently linked PAA NPs, commercially available CB was derivatized to an acrylamide-terminated form, by two-step reaction as summarized in **Scheme 1**. The two sulfonic acid groups were converted into sulfonyl chloride groups,[16] forming an intermediate (CB-I), and were then changed into sulfamide groups after reacting with *N*-(3-aminopropyl)methacrylamide (APMA) under basic conditions[17] to make CB-APMA. This modification was

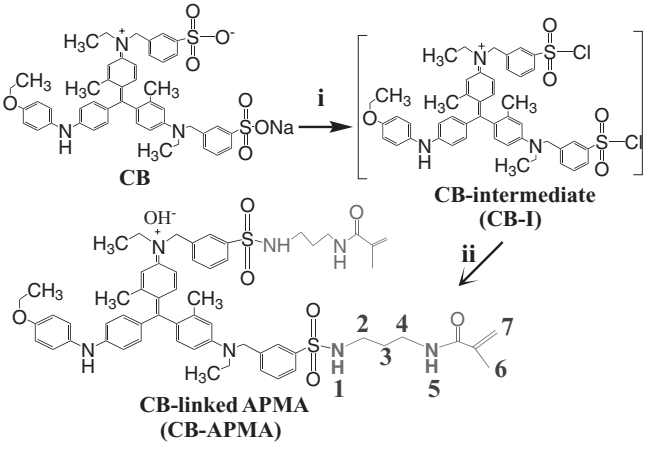

Scheme 1. Synthesis of CB-APMA: **i**) $POCl_3$, dimethylformamide (DMF), CH_2Cl_2, 40 °C, 7.5 h/≈20 °C, overnight; **ii**) APMA, dimethyl sulfoxide (DMSO), triethylamine, CH_2Cl_2, 0 °C, 30 min/≈20 °C, 1.5 h.

performed without separation of CB-I, which is moisture sensitive, but the identity of CB-I was confirmed by mass spectrometry showing a molecular ion at *m*/*z* 868.1. The color of CB and CB-APMA is bright blue, whereas that of CB-I is green. The CB-APMA was obtained in a dried powder form, with 68% yield, and had 97% purity by elemental analysis ($C_{61}H_{74}N_7O_7S_2^+(OH^-)_{0.6}(SO_4^{2-})_{0.2}$: C 64.04, H 6.58, N 8.58, O 11.75, S 6.17).

The CB-APMA was characterized by ^{1}H NMR (1D and 2D), mass, and IR spectrometric measurements. The NMR proton assignments for CB-APMA are listed as follows: ^{1}H NMR (CD_2Cl_2, 500 MHz): δ = 7.91–7.69 (m, 4H; Ar–H), 7.47 (t, J = 7.5 Hz, 2H; CONH), 7.43–7.34 (m, 3H; Ar–H), 7.34–7.26 (m, 3H; Ar–H), 7.25–7.18 (m, 2H; Ar–H), 7.17–7.10 (m, 2H; Ar–H), 7.04 (t, J = 6.5 Hz, 2H; SO_2–NH), 6.97–6.74 (m, 4H; Ar–H), 6.74–6.44 (m, 4H; Ar–H), 5.87–5.64 (m, 2H; CH_2=), 5.31–5.10 (m, 2H; CH_2=), 4.73(s, 4H; Ar–CH_2), 4.02 (q, J = 7 Hz, 2H; CH_3–CH_2–O), 3.85–3.49 (m, 4H; CH_3–CH_2–N), 3.49–3.41 (m, 4H; −CONH–CH_2–), 2.99–2.71 (m, 4H; SO_2NH−CH_2), 1.94–1.84 (m, 6H; CH_3–C=), 1.84–1.71 (br, 6H; CH_3–Ar), 1.70–1.54 (m, 4H; $CH_2CH_2CH_2$), 1.38 (t, J = 7 Hz, 3H; CH_3–CH_2–O), 1.30 ppm (t, J = 7 Hz, 6H; CH_3–CH_2–N). The identity of CB-APMA was also confirmed by the mass spectrum, which showed a molecular ion at *m*/*z* 1080.50. The IR (KBr) spectra confirmed the presence of amide C=O at 1654, CO–NH at 1605, C=CH at 1494, and SO_2–NH at 1166 cm^{-1}. (More detailed analysis data are available in the Supporting Information.)

2.2. Preparation of NPs Containing CB-APMA by Covalent Linkage

CB covalently linked PAA NPs were prepared by reverse microemulsion polymerization with monomer mixtures containing CB-APMA, acrylamide (monomer), APMA (comonomer), and glycerol dimethacrylate (GDMA, crosslinker; see Scheme S1, Supporting Information). CB-encapsulated and CB-post-loaded PAA NPs were also prepared for comparison (Scheme S1). The crosslinker, GDMA, contains hydrolyzable ester bonds, thus making the prepared NPs biodegradable in vivo.[11,18] APMA was included for providing the amine functionality to the NPs, so the NPs can be modified with F3 peptides and PEG units (Scheme S2, Supporting Information). The CB-APMA is insoluble in water and can also serve as a crosslinker as it has two polymerizable carbon double bonds (–C=C–). The inclusion of CB-APMA was found to greatly influence the formation of the NPs. Thus, the synthetic protocol for CB-linked PAA NPs had to be significantly modified from that of CB-encapsulated or CB-post-loaded PAA NPs. The monomers were dissolved in a DMF/water mixture. The amount (mole) of GDMA in the monomer mixture was reduced by the added amount of CB-APMA, which kept the amount of the crosslinkers the same as that used for typical PAA NPs. The amount of surfactants was increased by a factor of ≈3. Compared to preparing blank PAA NPs, about 16 times higher initiator quantities were required for the initiation of the polymerization, probably because of the significant quenching of the produced radicals by the larger amounts of dye and surfactant.

2.3. Surface Modifications and Cancer-Specific Targeting

To achieve brain-cancer-specific targeted delivery of CB-loaded PAA NPs, two surface modifications/conjugations were made. First, the surface of CB-loaded NPs was PEGylated (coated with polyethylene glycol) by using the heterobifunctional PEG, SCM-PEG-MAL, as a crosslinking reagent between the NP and a targeting moiety. Its amine-reactive terminal (succinimidyl carboxymethyl ester, SCM) chemically links to the primary amine group present on the surface of PAA NPs. Then, the sulfhydryl-reactive terminal (maleimidyl ester, MAL) binds to the sulfhydryl group in F3-Cys peptide for cancer targeting or to L-cysteine for control (Scheme S2). The surface charge in each modification step was measured as an indicator showing whether the product was formed as desired, using the dynamic light scattering (DLS) zeta potential measurement technique. Unmodified NPs exhibit a relatively strong positive charge (+17.38 ± 3.30 mV in zeta potential) due to the presence of protonated amine groups (-NH_3^+) on the surface. PEGylation on the surface resulted in a significantly reduced positive charge (+2.98 ± 1.40 mV). The coverage of PAA NPs by PEG was estimated to be about 40 PEG molecules per single PAA NP by UV/Vis absorption-based analysis done after treating the NPs with fluorescein-labeled PEG-succinimidyl ester. F3-conjugated NPs regained a net positive surface charge (+15.11 ± 2.36 mV) because of the strong basic amino acid composition of the F3 peptide.

The introduction of PEG in between the NP and the F3 peptide was another effort to improve in vivo tumor delineation efficacy, compared to the previous approach that utilized a relatively small molecular crosslinker, sulfo-SMCC.[13] Surface PEGylation can effectively suppress the nonspecific binding by the free motion of the electrically neutral, long polymer PEG chains, thereby allowing only target-specific binding to the cancer cells by the F3 peptide. Also, PEGylation can improve the colloidal stability (suspendability) of the NPs in physiological media, which results in longer plasma circulation times. Such effects should improve the in vivo function of the F3-targeted CB-linked PAA NPs.

2.4. NP Characterization

The scanning electron microscopy (SEM) and transmission electron microscopy (TEM) images show that the CB-linked NPs have spherical particulate morphology and a size of ≈45 nm in diameter, whereas the CB-encapsulated or CB-post-loaded NPs have a size of ≈30 nm (**Figure 2**). The average sizes (diameters) of CB-linked PAA NPs, CB-encapsulated PAA NPs, and CB-post-loaded PAA NPs in water, measured by DLS, are (86.8 ± 21.0), (57.3 ± 11.8) and (54.1 ± 10.2) nm, respectively, whereas for blank PAA NPs it is 53.4 ± 9.5 nm. The fact that the hydrodynamic sizes of these NPs are much larger than those determined by the electron micrographs indicates that the PAA NPs can swell in aqueous solution, manifesting a hydrogel characteristic. The average sizes of the F3-targeted and nontargeted (PEGylated) CB-linked PAA NPs are, respectively, (90.3 ± 7.1) and (88.6 ± 11.9) nm by DLS, which indicates that surface conjugation does not affect the particle

NANO MICRO small

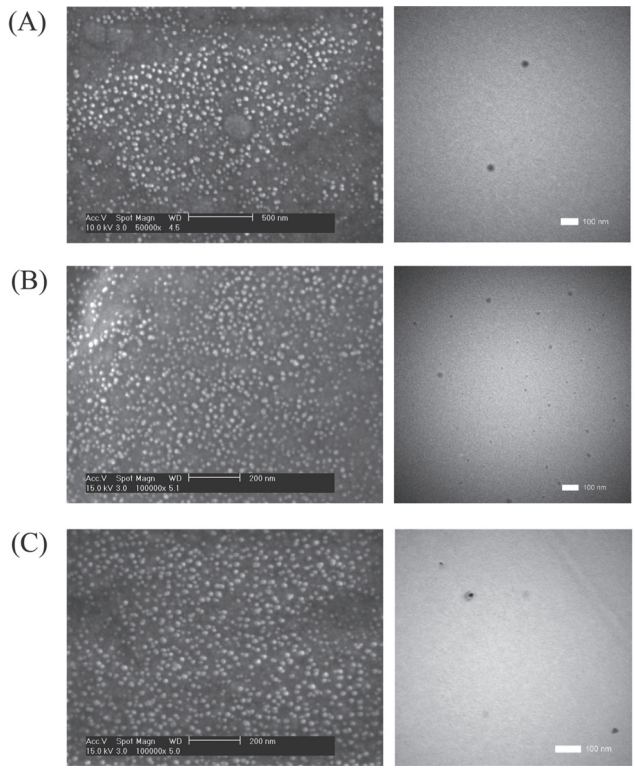

Figure 2. SEM and TEM images of the prepared NPs: A) CB covalently linked PAA NPs; B) CB-encapsulated PAA NPs; and C) CB-post-loaded PAA NPs.

size significantly. The size of all CB-loaded PAA NPs, before and after surface modification, falls into the range of 10–100 nm, which is generally the accepted optimal size range for in vivo applications, because a particle in this range is too large to undergo renal elimination and too small to be recognized by phagocytes.[19–21]

We also confirmed that various dye loading methods (post-loading and covalent linking) did not make recognizable differences in the zeta potential value. The amount of conjugated F3 peptide was determined to be 0.027 μmol mg^{-1} of NP by weight, by quantitative amino acid assays. We believe that F3 peptides are conjugated mostly to the surface through PEG crosslinker because of: 1) PEG molecules being mostly located on the surface, as shown by the significant surface charge reduction after PEGylation and the regaining of positive surface charge after F3 conjugation (Section 2.3); and 2) considering the relatively large molecular weight of the F3 peptide (3566 g mol^{-1}). Our previous studies show that molecules having molecular weights larger than ≈2500 Da do not leach out of PAA NPs, thus indicating that such molecules can hardly enter into the NPs from the outside.[22]

2.5. Quantification of Dye Loading Efficiency

The absorption spectra of CB-linked NPs in aqueous solution show that their absorption maximum is observed at 610 nm while that of CB-free dye in aqueous solution is at 597 nm (Supporting Information). Just as for the solvent-dependent spectral shifts of the dyes,[23] such a peak shift may be due to a polarity and polarizability of the CB-linked NP matrix that differs from that of water or that of the normal PAA NP matrix. CB has a peak at 618 nm when dissolved in DMF. The observed peak shift does not produce significant visible color changes (Supporting Information).

The loading of CB per NP is an important factor for successful visible color-based tumor delineation. In our studies with CB-free dye, the estimated dose for obtaining a sufficient color delineation effect in a rat brain tumor window (BTW) model was about 70 mg kg^{-1}, although the color contrast started to fade at about 60 min after injection.[9] The required CB dose for the CB-loaded NPs may be lower than the CB-free dye dose, through the expected enhancement in effectivity due to passive delivery by the EPR effect, the surface-conjugated PEG, and the tumor-specific targeting moieties. We aimed at using half of the free CB dose, that is, 35 mg kg^{-1}, for CB-loaded NPs. According to our previous in vivo animal studies, the PAA NPs showed no evidence of alterations in histopathology or clinical chemistry values at doses of 10 mg kg^{-1} to 1 g kg^{-1}.[11] We chose the maximum NP dose to be equal to or less than 500 mg kg^{-1}. To match the dose requirement for the CB dye and the NPs, the CB loading per NP should be at least ≈7 wt%. Among the three types of CB-loaded PAA NPs, the CB-encapsulated PAA NPs showed the worst CB loading efficiency, achieving only about 0.5 wt% loading of CB per NP, at most, and this sample was excluded from further studies. The CB-post-loaded PAA NPs were obtained with high dye contents (up to 9%), with >90% of loading efficiency, which were controlled by the input amount of CB. The CB loading efficiency within CB-linked NPs was also high (ca. 70%) and controlled by the input amount of CB-APMA. A CB loading of up to 14 wt% was achieved for the CB-linked NPs.

2.6. Dye Leaching under Simulated Physiological Conditions

Dye leaching tests were performed for the CB covalently linked PAA NPs and the CB-post-loaded PAA NPs after being incubated in a pH 7.4 phosphate-buffered saline (PBS) solution containing 9% bovine serum albumin (BSA) at 37 °C (mimicking the composition of a physiological fluid) for 2 h and by measuring the CB content in the filtrate separated from the NPs by centrifugal filtration. There was significant leaching of CB out of the CB-post-loaded PAA NPs (60 ± 9%), but no detectable leaching of CB out of the CB-linked NPs. The high dye leaching out of the CB-post-loaded NPs may be attributed to the dye loading being achieved by physical interactions, namely electrostatic or hydrophobic interactions, between the dye and the NPs. The latter are thus easily affected by the surrounding environment, which can render even stronger interactions. This characteristic represents a crucial drawback of the post-loaded dye NPs when the aim is in vivo tumor delineation. As shown by the above results, the covalent linkage of the CB molecule to the NP matrix polymer backbone completely eliminates dye leaching, so that the entire dye content can be delivered to the tumor with the targeted NPs.

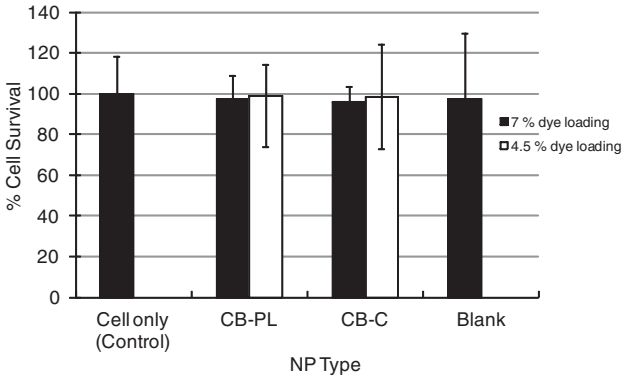

Figure 3. Examination of cytotoxicity of CB-loaded PAA NPs. Compared to the cell-only control, none of the three kinds of NPs, CB-post-loaded NPs (CB-PL), CB-linked NPs (CB-C), and blank PAA NPs, showed a statistically meaningful reduction in the cell survival rate, thus indicating negligible cytotoxicity. Dye loading differences (7 and 4.5%) also showed only negligible differences in cell viability.

2.7. Cytotoxicity Examination by MTT Assay

The potential toxicity of the CB-loaded NPs was tested by an MTT assay. As displayed in **Figure 3**, cell survival rates did not show noticeable differences among CB-post-loaded NPs, CB covalently linked NPs, blank NPs, and the control (cells only). The average cell survival rates were higher than 96% in all cases, regardless of the NP type and dye content. This result clearly shows that the PAA NP matrix, with or without CB dye loading, does not cause significant cytotoxic effects and thus may be readily deployed for *intraoperative* in vivo applications.

2.8. In vitro Cell Staining

Based on the effective suppression of dye leaching, we performed in vitro cell staining experiments on 9L gliosarcoma cells, using F3-conjugated or nontargeted PAA NPs (PEGylated control NPs) containing 7 wt% CB by covalent linking, as previously described.[13] While F3-conjugated CB-linked NPs could effectively stain the 9L cell pellet to a noticeable blue color, under identical conditions the nontargeted counterparts induced a negligible blue staining effect (**Figure 4**). Note that in the case of CB-post-loaded NPs, even the nontargeted ones caused significant tumor cell staining (Figure 1).[13] This suggests that the amount of CB dye that remained within the CB-post-loaded NPs may decrease significantly by the leaching out of dye molecules when the NPs reach the tumor, and that the leached-out free dye may cause nonspecific staining of other tissues, thus limiting their use in vivo. Meanwhile, the CB-linked NPs, which showed no premature dye leaching, are expected to provide stronger and longer-lasting tumor delineations in vivo.

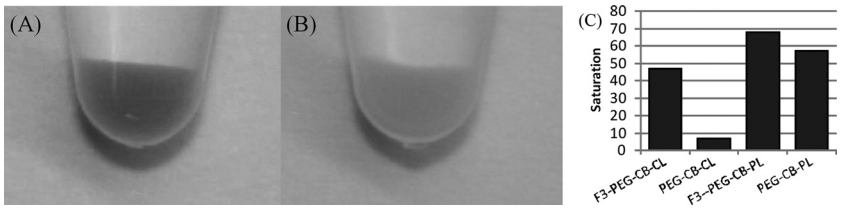

Figure 4. In vitro cell staining by A) F3-targeted CB-linked NPs, B) nontargeted CB-linked NPs after 1 h of incubation, and C) comparison of blue staining by saturation analysis.[9,13] The F3-targeted CB-linked NPs caused a clear blue staining effect whereas the nontargeted control caused a negligible effect.

2.9. In vivo Tumor Delineation

Based on the aforementioned improvements, an in vivo tumor delineation study was performed in a rat BTW model,[9] that is, rats with implanted 9L gliosarcoma and with a glass cranial window, so that the in vivo tumor delineation could be evaluated in real time by visual observation through the window, as previously described.[9] **Figure 5** shows representative pictures of the tumors in the BTW models at 0, 60, and 120 min after injection of the three kinds of 7 wt% CB-loaded NPs—F3-targeted and nontargeted CB-linked PAA NPs, and nontargeted CB-post-loaded PAA NPs—at an NP dose of 500 mg kg^{-1}. The tumor margin that was poorly defined before administration of the NPs becomes readily apparent after administration of any of the three CB-loaded NPs. As shown in Figure 5, the relative strengths of visual delineation induced by the NPs were in the order: F3-targeted CB-linked NPs > nontargeted CB-linked NPs > nontargeted CB-post-loaded NPs. The reason that nontargeted NPs exhibited tumor-specific accumulation, though to a weaker extent, can be explained as being a consequence of passive targeting by the EPR effect. In spite of the same dye content (7%), the nontargeted CB-post-loaded NPs showed a significantly reduced delineation effect compared to the nontargeted CB-linked NPs. This reduction is attributed to the loss of CB content in the post-loaded NPs, due to dye leaching; this is borne out by the decreasing contrast with time (Figure 5). The F3-targeted, CB-linked NPs showed the strongest tumor delineation effect of all the samples, and this enhancement is attributed to the additive effects of 1) active targeting by the F3 peptide, 2) passive targeting by the EPR effect, and 3) no loss of dye content. These results clearly manifest the advantage of F3-targeted CB-linked NPs for tumor-selective delineation. Also, the progress of tumor delineation contrast over time reveals further evidence of the improvement due to the covalent attachment of the CB dye to the NP matrix. The color of the tumors treated by both F3-targeted and nontargeted CB-linked NPs became stronger with time (up to 120 min). However, the tumor staining by the nontargeted CB-post-loaded NPs started to fade after 60 min. In our previous study with free CB dye, we also observed such early clearance of the color from the tumor.[9] This again indicates that the CB may keep leaching out of the CB-post-loaded NPs, thus resulting in less efficient tumor delineation. Currently, kinetics and dose-dependency studies with F3-targeted and nontargeted CB-linked NPs are ongoing, to evaluate the optimal doses of NPs and CB as well as the efficiency of the F3 targeting over time.

NANO MICRO small

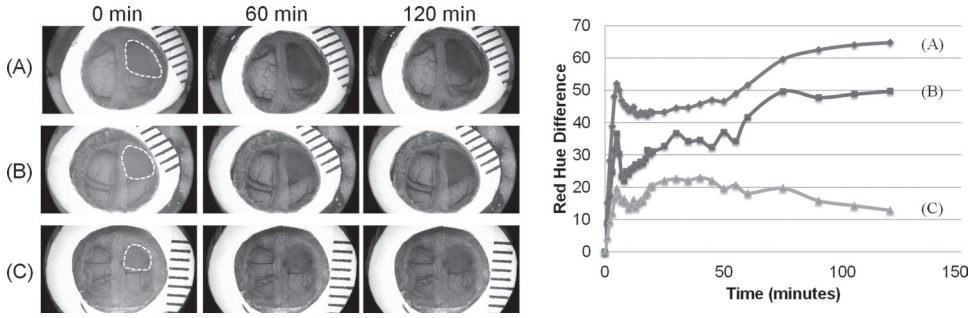

Figure 5. Left: Photographs of representative tumors in BTW models, at 0, 60, and 120 min after administration of A) F3-targeted CB-linked NPs, B) nontargeted CB-linked NPs, and C) nontargeted CB-post-loaded NPs. The tumor margin in each animal was marked by a white dashed line on the initial (0 min) images. The F3-targeted CB-linked NPs (A) localize within the tumor, thus enabling an obvious visual delineation from the surrounding normal brain, whereas nontargeted control (B) and nontargeted CB-post-loaded control NPs (C) result in a noticeably inferior delineation effect. This degree of delineation would improve the ability of surgeons to distinguish tumor from normal brain under standard lighting conditions. Right: Colorimetric analysis results with ImageJ software,[9,13] to quantify the degree of color change in the tumor. The difference in red hue is the best method to reflect the visual difference between tumor and normal brain.

3. Conclusion

We have demonstrated the preparation of tumor-targeted, intensely blue colored NP agents for tumor-specific visible color contrast, designed to aid in intraoperative tumor margin delineation. The color contrast agent is made of PAA hydrogel NPs that are covalently linked with CB dye, by copolymerizing the CB-linked acrylamide (CB-APMA) that was synthesized for this purpose. The CB covalently linked PAA NPs have the advantages of 1) good suspension capability in aqueous solutions and 2) no leaching of the color contrast ingredient. These NP agents, through the attachment of PEG and F3 peptide, enable efficient and lasting in vivo tumor targeting by the dye. The selective and visible tumor staining ability was confirmed both in cells (in vitro) and in a 9L tumor-bearing rat model (in vivo). The tumor-targeting blue colored NP agents are likely to enable color-guided tumor resection in real time, without the need for extra equipment, special lighting conditions, or surgery interruptions.

4. Experimental Section

Materials: Coomassie Blue G (CB), triethylamine (TEA), dichloromethane, acrylamide (AA), glycerol dimethacrylate (GDMA), ammonium persulfate (APS), *N*,*N*,*N*′,*N*′-tetramethylethylenediamine (TEMED), sodium dioctyl sulfosuccinate (AOT), Brij 30, hexane, *N*,*N*-dimethylformamide (DMF), dimethyl sulfoxide (DMSO), L-cysteine, Dulbecco's modified Eagle's medium (DMEM), Rosewell Park Memorial Institute medium (RPMI-1640), and 3-(4,5-dimethylthiazol-2-yl)-2,5-diphenyltetrazolium bromide (MTT) were purchased from Sigma Aldrich. Phosphorus oxychloride, petroleum ether (40 to 60 °C), and toluene were purchased from Acros Organics. *N*-(3-Aminopropyl)methacrylamide hydrochloride (APMA) was purchased from Polysciences Inc. Ethanol (95%), anhydrous ethyl ether, and hexane were purchased from Fisher Scientific. Anthracene-9,10-dipropionic acid, disodium salt (ADPA) was purchased from Molecular Probes. Fluorescein isothiocyanate (FITC) was purchased from Thermo Scientific. Bovine serum albumin (BSA, 30%) was purchased from United States Biological Corporation. Phosphate-buffered saline (PBS) solution (pH 7.4) was made with phosphate-buffered saline tablet from Sigma Aldrich. F3-Cys peptide (KDEPQRRSARLSAKPAPPKPEPKPKKAPAKKC) was purchased from SynBioSci. A heterobifunctional polyethylene glycol (MAL-PEG-NHS, 2k) was purchased from Creative PEGWorks. Six-well cell culture plates and 96-well microplates were purchased from BD Biosciences. The water used throughout the experiments was deionized (DI) water, purified by a Milli-Q system from Millipore Co.

Synthesis of CB-APMA: CB (8.54 g, 90% purity commercial CB) was added to a 500 mL dry round-bottom flask containing DMF (70 mL). After sonication, dichloromethane (200 mL) was added to the dye solution followed by phosphorus oxychloride (32 mmol). The mixture was refluxed for 7.5 h at ≈40 °C and then cooled to room temperature overnight. The reaction mixture was cooled in an ice water bath, filtered into a suction flask containing APMA (25 mmol) in DMSO (10 mL), dichloromethane (50 mL), and TEA (153 mmol) in an ice water bath, and then stirred for 1.5 h at room temperature. Petroleum ether (500 mL) was added to the suction flask to precipitate the blue dye. The oily dye residue was dissolved in dichloromethane (200 mL), and toluene (500 mL) was added to precipitate the blue dye. The precipitate was filtered under vacuum, and then washed with ethyl ether to obtain a dry powder. Abundant DI water was added to wash the dry product to eliminate the water-soluble impurities. After vacuum drying, the product was dissolved in dichloromethane (200 mL) in a beaker and the mixture was stirred. DI water (200 mL) and subsequently ethyl ether (280 mL) were added to the mixture with stirring for ≈10 min and then the solution was allowed to stand for 2–8 h. The solvents were decanted, vacuum filtered, then the product was dried in a vacuum oven. The product was recrystallized from dichloromethane. An iridescent red-violet crystalline powder (6.8 g), CB-APMA hydroxide (see Scheme 1), was obtained with 68% yield and 97% purity.

Preparation of CB-Loaded NPs: CB Covalently Linked PAA NPs: CB covalently linked PAA NPs were prepared by a reverse microemulsion polymerization method. A monomer solution was prepared by dissolving acrylamide (610 mg) and APMA (45 mg) in water (1 mL). A dye solution was prepared by dissolving CB-APMA (100 mg) in DMF (0.4 mL) and then GDMA (360 μL) was added to the dye solution. The monomer solution was added to the mixture and then it was stirred and sonicated to make a homogeneous solution. The prepared CB-containing monomer solution

was added to deoxygenated hexane (120 mL) that contained two surfactants, AOT (3.9 g) and Brij 30 (10.3 mL). After stirring the mixture under an inert atmosphere for 20 min, a freshly prepared 50% (w/v) APS solution (240 μL) and TEMED (150 μL) were added to initiate polymerization. The solution was then stirred under an inert atmosphere at room temperature for 1 h. After completion of the polymerization, hexane was removed with a rotary evaporator and the residue was made into a suspension by adding ethanol. The suspension was subjected to a washing procedure in an Amicon filtration system (Millipore Co.) with a 500 kDa filter membrane under 10–20 psi of pressure. The washing procedure was carried out with ethanol ten times and with water ten times, during which surfactants and unreacted molecules were removed from the product. The resultant CB covalently linked NPs were obtained through a freeze-drying process.

Preparation of CB-Loaded NPs: CB-Encapsulated PAA NPs: CB-encapsulated PAA NPs were prepared by a reverse microemulsion polymerization method. A CB-containing monomer solution was prepared by dissolving acrylamide (711 mg), APMA (55 mg), and CB (100 mg) in water (1.4 mL). GDMA (470 μL) was added to the mixture and then it was stirred and sonicated to make a homogeneous solution. The mixture solution was added to deoxygenated hexane (120 mL) that contained two surfactants, AOT (3.9 g) and Brij 30 (10.3 mL). After stirring the mixture under an inert atmosphere for 20 min, a freshly prepared 50% (w/v) APS solution (240 μL) and TEMED (150 μL) were added to initiate polymerization. The solution was then stirred under an inert atmosphere at room temperature for 1 h. After completion of the polymerization, hexane was removed with a rotary evaporator and the residue was made into a suspension by adding ethanol. The suspension was subjected to a washing procedure in an Amicon filtration system (Millipore Co.) with a 500 kDa filter membrane under 10–20 psi of pressure. The washing procedure was carried out with ethanol ten times and with water ten times, during which surfactants and unreacted molecules were removed from the product. The resultant CB-encapsulated NPs were obtained through a freeze-drying process.

Preparation of CB-Loaded NPs: *CB-Post-Loaded PAA NPs*: For the post-loading of CB, blank PAA NPs were prepared by a reverse microemulsion polymerization method. A monomer solution was prepared by dissolving acrylamide (711 mg) and APMA (55 mg) in water (1.3 mL). GDMA (470 μL) was added to the monomer solution and then the mixture was stirred and sonicated to make a homogeneous solution. The mixture solution was added to deoxygenated hexane (45 mL) that contained two surfactants, AOT (1.6 g) and Brij 30 (3.3 mL). After stirring the mixture under an inert atmosphere for 20 min, a freshly prepared 10% (w/v) APS solution (100 μL) and TEMED (100 μL) were added to initiate polymerization. The solution was then stirred under an inert atmosphere at room temperature for 2 h. After completion of the polymerization, hexane was removed with a rotary evaporator and the residue was made into a suspension by adding ethanol. The suspension was subjected to a washing procedure in an Amicon filtration system (Millipore) with a 300 kDa filter membrane under 10–20 psi of pressure. The washing procedure was carried out with ethanol ten times and with water ten times, during which surfactants and unreacted molecules were removed from the product. The resultant blank PAA NPs were obtained through a freeze-drying process.

The blank PAA NPs (50 mg) prepared were dispersed in water (5 mL). CB aqueous solution (1 mL, 5 mg mL^{-1}) was added under stirring and the mixture was stirred for 2 h at room temperature. With an Amicon centrifugal filter (Millipore, 100 kDa), a rinsing procedure was carried out by centrifugation at 5000 *g* for 20 min. During washing, the unloaded dye in the mixture solution was removed through a membrane. This procedure was repeated five times. The CB-post-loaded PAA solution was collected with a concentration of 20 mg mL^{-1}.

Preparation of F3-Targeted CB-Loaded PAA NPs: CB covalently linked PAA NPs (50 mg) or CB-post-loaded PAA NPs were dissolved in PBS (2.5 mL, pH 7.4). NHS-PEG-MAL (4 mg), a bifunctional conjugating polyethylene glycol, was added to the NP solution and the mixture was stirred for 30 min. With an Amicon centrifugal filter (Millipore, 100 kDa), a rinsing procedure was carried out by centrifugation at 5000 *g* for 20 min. During washing, unreacted molecules in the mixture solution were removed through a membrane. This procedure was repeated three times. The NP solution was reconstituted in PBS to 20 mg mL^{-1}, and F3-Cys peptide (2 μmol) was added. The mixture was stirred overnight at room temperature. L-Cysteine aqueous solution (63 μL, 10 mg mL^{-1}) was added and the mixture was stirred for 2 h to deactivate the functional ends of PEG unreacted with the peptides. The resultant F3-targeted CB-loaded PAA NPs were obtained after additional washing with repetitive centrifugation.

Preparation of Nontargeted CB-Loaded PAA NPs: CB covalently linked PAA NPs (50 mg) or CB-post-loaded PAA NPs were dissolved in PBS (2.5 mL, pH 7.4). NHS-PEG-MAL (4 mg), a bifunctional conjugating polyethylene glycol, was added to the NP solution and the mixture was stirred for 30 min. With an Amicon centrifugal filter (Millipore, 100 kDa), a rinsing procedure was carried out by centrifugation at 5000 *g* for 20 min. During washing, unreacted molecules in the mixture solution were removed through a membrane. This procedure was repeated three times. The NP solution was collected with a concentration of 20 mg mL^{-1}. L-Cysteine aqueous solution (125 μL, 10 mg mL^{-1}) was added and the mixture was stirred for 2 h. The resultant nontargeted CB-loaded PAA NPs were obtained after additional washing with repetitive centrifugation.

Dye Leaching Tests: CB-loaded PAA NPs (10 mg), CB covalently linked or CB-post-loaded, were dissolved in PBS (1.4 mL, pH 7.4). A BSA solution (0.6 mL, 30%) was added to the NP solution and the mixture was stirred for 2 h at 37 °C. The mixture was diluted by adding PBS (6 mL, pH 7.4) and filtered in an Amicon filtration system (Millipore) with a 500 kDa filter membrane under 10–20 psi of pressure. The first filtrate was collected with a volume of 5 mL and then PBS (6 mL, pH 7.4) was added to the Amicon container for the second filtration. Repeatedly, three filtrates were obtained with a volume of 5 mL. The filtrates were checked for their absorption with a UV/Vis spectrometer to characterize the dye leaching from the NPs.

Cell Culture: The human breast adenocarcinoma cell line MCF-7 and rat gliosarcoma cell line 9L were cultivated in RPMI-1640 with heat-inactivated fetal bovine serum (10%). The cells were plated on the glass coverslips in six-well plates for confocal microscopy imaging and 96-well plates for MTT cell viability assay.

MTT Cell Viability Assay: The cytotoxicity induced by the PAA NP matrix with various CB loadings—CB-post-loaded (7 and 4.5 wt% dye content), CB covalently linked (7 and 4.5 wt% dye content), or without CB (blank)—as well as cells without NPs (control), was evaluated by MTT cell viability assay that examines metabolic activity. 9L cells were plated on a 96-well plate with cell density

NANO MICRO small

of 5000 cells well^{-1} and cultivated overnight. Each type of NP was added to the wells (at 1 mg mL^{-1}) and incubated with the cells for 1 h. The cell medium was carefully replaced with MTT-containing medium (0.5 mg mL^{-1}) and cells were further incubated for 4 h. Then, the cell medium was aspirated gently and DMSO (200 μL) was added to each well to solubilize the formazan crystals produced from MTT in viable cells. After overnight rocking of the plate, the visible absorption at a wavelength of 550 nm of each well was measured with a Molecular Devices Spectramax Plus 384 plate reader. Results from 12 wells for each NP matrix were averaged.

In vitro Cell Staining by Visible Colorimetry: Four kinds of CB-loaded NPs containing an equal amount of CB were prepared for the tests: F3-targeted CB-linked PAA NPs, nontargeted CB-linked PAA NPs, F3-targeted CB-post-loaded NPs, and nontargeted CB-post-loaded NPs. 9L cells were cultivated for several days until they reached sufficient confluency. The cells were lifted off the bottom of a Petri dish by trypsinization and centrifuged to obtain a cell pellet (2000 rpm for 5 min). The supernatant was removed from the centrifuge tube to get rid of the trypsin and the cell pellet was resuspended in fresh colorless RPMI-1640 medium. The number of cells was counted with a hemacytometer and four centrifuge tubes containing cell suspensions of 5×10^6 cells were prepared. The cell suspension was incubated with each NP at 0.5 mg mL^{-1} for 1 h. Then, the cell suspension was centrifuged to obtain a cell pellet (2000 rpm for 5 min) to remove unbound NPs. The supernatant was taken from each tube carefully, so as not to disturb the pellet. A picture of each cell pellet was taken with a digital camera to show the degree of blue staining.

In vivo Tumor Delineation Study: The in vivo tumor delineation was performed in a rat brain tumor model that was prepared as previously described.[8] Briefly, biparietal craniectomies were performed on 8-week-old Sprague–Dawley rats. 9L glioma cells were injected intraparenchymally. A coverslip was bonded to the cranial defect with cyanoacrylate glue. When the tumor radius reached 1–2 mm, CB-loaded NPs were administered intravenously while the appearance of the cortical surface was recorded.

Supporting Information

Supporting Information is available from the Wiley Online Library or from the author. It includes detailed experimental procedures and analyses; NMR (CB, CB-APMA), IR (CB-APMA), mass spectra (CB, CB-I, CB-APMA), and elemental analysis (CB-APMA); absorption spectra of CB and CB-linked PAA NPs; and schemes for NP preparation and surface targeting.

Acknowledgements

This work was supported by Grants R33CA125297-R33CA125297-03s1, R01 EB007977, and R01 EB007977-02s1 (RK) and Guangxi Education Department (201102ZD031, GN).

[1] L. Rogers, J. Pueschel, R. Spetzler, W. Shapiro, S. Coons, T. Thomas, B. Speiser, *J. Neurosurg.* **2005**, *102*, 629–636.
[2] a) N. Sanai, M. S. Berger, *Neurosurgery* **2008**, *62*, 753–764; b) S. S. Lo, K. H. Cho, W. A. Hall, W. L. Hernandez, R. J. Kossow, C. K. Lee, H. B. Clark, *Int. J. Cancer* **2001**, *96*, 71–78; c) G. J. LaValle, D. A. Martinez, D. Sobel, B. DeYoung, E. W. Martin, *Surgery* **1997**, *122*, 867–871.
[3] P. W. A. Willems, M. J. B. Taphoorn, H. Burger, J. W. B. van der Sprenkel, C. A. Tulleken, *J. Neurosurg.* **2006**, *104*, 360–368.
[4] C. Nimsky, O. Ganslandt, H. Kober, M. Buchfelder, R. Fahlbusch, *Neurosurgery* **2001** , *48*, 1082–1089.
[5] J. Shinoda, H. Yano, S. I. Yoshimura, A. Okumura, Y. Kaku, T. Iwama, N. Sakai, *J. Neurosurg.* **2003**, *99*, 597–603.
[6] a) W. Stummer, S. Stocker, S. Wagner, H. Stepp, C. Fritsch, C. Goetz, A. E. Goetz, R. Kiefmann, H. J. Reulen, *Neurosurgery* **1998**, *42*, 518–525; b) W. Stummer, A. Novotny, H. Stepp, C. Goetz, K. Bise, H. J. Reulen, *J. Neurosurg.* **2000**, *93*, 1003–1013.
[7] G. W. Britz, S. Ghatan, A. M. Spence, M. S. Berger, *J. Neuro-Oncol.* **2002**, *56*, 227–232.
[8] T. Ozawa, G. W. Britz, D. H. Kinder, A. M. Spence, S. VandenBerg, K. R. Lamborn, D. F. Deen, M. S. Berger, *Neurosurgery* **2005**, *57*, 1041–1046.
[9] D. A. Orringer, T. Chen, D. L. Huang, W. M. Armstead, B. A. Hoff, Y. E. L. Koo, R. F. Keep, M. A. Philbert, R. Kopelman, O. Sagher, *Neurosurgery* **2010**, *66*, 736–743.
[10] D. A. Hansen, A. M. Spence, T. Carski, M. S. Berger, *Surg. Neurol.* **1993**, *40*, 451–456.
[11] Y. E. L. Koo, G. R. Reddy, M. Bhojani, R. Schneider, M. A. Philbert, A. Rehemtulla, B. D. Ross, R. Kopelman, *Adv. Drug Delivery Rev.* **2006**, *58*, 1556–1577.
[12] a) O. Veiseh, C. Sun, C. Fang, N. Bhattarai, J. Gunn, F. Kievit, K. Du, B. Pullar, D. Lee, R. G. Ellenbogen, J. Olson, M. Zhang, *Cancer Res.* **2009**, *69*, 6200–6207; b) O. Veiseh, C. Sun, J. Gunn, N. Kohler, P. Gabikian, D. Lee, N. Bhattarai, R. Ellenbogen, R. Sze, A. Hallahan, J. Olson, M. Zhang, *Nano Lett.* **2005**, *5*, 1003–1008; c) M. Kircher, U. Mahmood, R. S. King, R. Weissleder, L. Josephson, *Cancer Res.* **2003**, *63*, 8122–8125.
[13] D. A. Orringer, Y. E. L. Koo, T. Chen, G. Kim, H. J. Hah, H. Xu, S. Wang, R. Keep, M. A. Philbert, R. Kopelman, O. Sagher, *Neurosurgery* **2009**, *64*, 965–971.
[14] H. J. Chial, H. B. Thompson, A. G. Splittgerber, *Anal. Biochem.* **1993**, *209*, 258–266.
[15] S. H. Taylor, J. P. Shillingford, *Brit. Heart J.* **1959**, *31*, 497–504.
[16] S. Fujita, *Synthesis* **1982**, 423–424.
[17] S. G. Jarboe, M. S. Terrazas, P. Beak, *J. Org. Chem.* **2008**, *73*, 9627–9632.
[18] S. J. Holland, B. J. Tighe, P. L. Gould, *J. Controlled Release* **1986**, *4*, 155–180.
[19] S. M. Moghimi, A. C. Hunter, J. C. Murray, *Pharmacol. Rev.* **2001**, *52*, 283–318.
[20] S. M. Moghimi, B. Bonnemain, *Adv. Drug Delivery Rev.* **1999**, *37*, 295–312.
[21] R. Weissleder, J. F. Heautot, B. K. Schaffer, N. Nossiff, M. I. Papisov, A. A. Bogdanov, T. J. Brady, *Radiology* **1994**, *191*, 225–230.
[22] Y. Koo Lee, E. E. Ulbrich, G. Kim, H. Hah, C. Strollo, W. Fan, R. Gurjar, S. M. Koo, R. Kopelman, *Anal. Chem.* **2010**, *82*, 8446–8455.
[23] C. Reichardt, in *Solvents and Solvent Effects in Organic Chemistry*, 2nd ed., VCH, Weinheim **1988**.

Received: August 8, 2011
Revised: November 11, 2011
Published online: January 9, 2012

